Chapter 5

Surface plasmons and gain media

by

M.A. Noginov, G. Zhu

Center for Materials Research, Norfolk State University, Norfolk, VA, 23504

V.P. Drachev, V.M. Shalaev

School of Electrical & Computer Engineering and Birck Nanotechnology Center, Purdue University, West Lafayette, IN 47907

Nanophotonics with Surface Plasmons
Advances in Nano-Optics and Nano-Photonics
ISSN: 1871-0018

V.M. Shalaev & S. Kawata (Editors)

DOI: 10.1016/S1871-0018(06)02005-X

Contents

§ 1. Introduction

The technique of coloring stain glasses by gold and silver nanoparticles was known to Romans. The British Museum has a famous Lycurgus Cup (4th Century A.D.), which changes its color depending on the illumination (fig. 1). When viewed in reflected light, for example, in daylight, it appears green. However, when a light is shone into the cup and transmitted through the glass, it appears red. Nowadays it is known that the coloration of the Cup is determined by the frequency of localized surface plasmon (SP) resonance in metallic nanoparticles embedded into the glass.

Localized SP is the oscillation of free electrons in a metallic particle (driven by an external electromagnetic wave), whose resonance frequency is the plasma frequency adjusted by the size and, mainly, the shape of the particle. A phenomenon relevant to localized SPs is a surface plasmon polariton (SPP) or a surface electromagnetic wave propagating along the interface between two media possessing permittivities with opposite signs, such as metal–dielectric interface. The plasmon's electromagnetic field is concentrated in the close vicinity to the surface of the particle or metal–dielectric boundary.

Fig. 1. Lycurgus Cup (4th Century A.D.) at different illuminations.

Localized plasmons are found on rough surfaces (Ritchie, 1973; Fleischmann et al., 1974; Moskovits, 1985), in engineered nanostructures (Quinten et al., 1998; Averitt et al., 1999; Brongersma et al., 2000; Mock et al., 2002; Pham et al., 2002), as well as in clusters and aggregates of nanoparticles (Kreibig and Vollmer, 1995; Quinten, 1999; Su et al., 2003). In the spots where local fields are concentrated, both linear and nonlinear optical responses of molecules and atoms are largely enhanced. This leads to a number of important applications, the most matured of which is the surface enhanced Raman scattering (SERS) (Fleischmann et al., 1974).

SPs result in enhanced local fields and, thus, can dramatically enhance the Raman signal, which depends linearly on the local field intensity. Among other advantages, SERS makes possible rapid molecular assays for detection of biological and chemical substances (Kneipp et al., 2002). A very high sensitivity of SERS enables observation of Raman scattering from a single molecule attached to a metal colloidal particle (Kneipp et al., 1997; Nie and Emory, 1997).

Raman scattering sensing techniques can not only detect the presence of a biomolecular analyte, but also provide a great deal of information on exactly what specific molecules are being detected. SERS enables molecular "fingerprinting," which is of particular interest for molecule sensing and bio-applications. A detailed analysis of this very powerful sensing technique is outside the scope of this chapter. We mention here only some recently developed, particularly efficient and sensitive SERS substrates. Those include nanoshells developed by the Halas group (Prodan et al., 2003), substrates fabricated with nanosphere lithography developed in the Van Duyne group (Hayes and Van Duyne, 2003), and adaptive silver films developed by Drachev et al. (2004).

Fractal aggregates of metallic nanoparticles supporting localized SPs can lead to extremely large enhancements of local field amplitudes exceeding those of single metallic particles (Markel et al., 1996; Shalaev et al., 1996; Shalaev, 2000). A number of interesting optical phenomena (such as highly efficient harmonic generation, SERS, Kerr effect, etc.) caused by dramatic field enhancement in hot spots of fractal aggregates of silver nanoparticles have been theoretically predicted and experimentally demonstrated by Shalaev and co-workers (Shalaev, 1996; Shalaev, 2000; Shalaev, 2002). We note that a fractal aggregate can be roughly thought of as a collection of spheroids, with different aspect ratio, formed by various chains of nanoparticles in the aggregate (Shalaev, 2000).

Brus and Nitzan (1983) proposed to use gigantic localized fields to influence photochemistry of reactions. Later this phenomenon was studied in application to photocells, detectors, and other processes including

vision (Hutson, 2005). The enhancement of the response of a p-n junction by localized SPs has been studied recently (Schaadt et al., 2005). A strong field enhancement in the vicinity of metallic tip enables linear and nonlinear near-field scanning microscopy, spectroscopy, and photomodification with nanoscale resolution (Stockman, 1989; Ferrell, 1994; S'anchez et al., 1999). An extraordinary high transmission of light through periodic arrays of subwavelength holes in metallic films has been explained in terms of resonant excitation of SPs by Ghaemi et al. (1998). An enhancement of surface magneto-optical interaction by SPs has been discussed by Bonod et al. (2004).

Negative-index materials (NIMs) have a negative refractive index, so that the phase velocity is directed against the flow of energy. There are no known naturally occurring NIMs in the optical range. However, artificially designed materials (metamaterials) can act as NIMs. Metamaterials can open new avenues to achieving unprecedented physical properties and functionality unattainable with naturally existing materials, as was first described by Veselago in his seminal paper (Veselago, 1968). Optical NIMs (ONIMs) promise to create entirely new prospects for controlling and manipulating light, optical sensing, and nanoscale imaging and photolithography.

Proof-of-principle experiments (Smith et al., 2000; Shelby et al., 2001) have shown that metamaterials can act as NIMs at *microwave* wavelengths. NIMs drew a large amount of attention after Pendry predicted that a NIM can act as a superlens, allowing an imaging resolution which is limited not by the wavelength but rather by material quality (Pendry, 2000). The near-field version of the superlens has recently been reported by the Zhang and Blaikie groups (Fang et al., 2005; Melville, and Blaikie, 2005).

While negative permittivity $\varepsilon' < 0$ ($\varepsilon = \varepsilon' + i\varepsilon''$) in the optical range is easy to attain for metals, there is no magnetic response for naturally occurring materials at such high frequencies. Recent experiments showed that a magnetic response and negative permeability $\mu' < 0$ ($\mu = \mu' + i\mu''$) can be accomplished at terahertz frequencies (Linden et al., 2004; Yen et al., 2004; Zhang et al., 2005). These studies showed the feasibility of ONIMs because a magnetic response is a precursor for negative refraction. The metamaterial with a negative refractive index at 1.5 μm, based on paired metal nanorods embedded in a dielectric, was designed (Podolskiy et al., 2002, 2003, 2005) and experimentally demonstrated by the Shalaev group (Shalaev et al., 2005; Drachev et al., 2006; Kildishev et al., 2006).

Metallic surfaces and nanoparticles can influence not only nonlinear but also linear optical responses. Thus, the dependence of emission spectra and emission lifetimes of luminescent centers on (submicron) distance

from a metallic mirror has been discussed in detail in review by Drexhage (1974) and references therein. An increase of luminescence intensity of dye molecules *adsorbed* onto islands and films of metal nanoparticles, when the plasma resonances are coupled to the absorption spectra of the molecules, has been observed in the early 80s by Glass et al. (1980, 1981) and Ritchie and Burstein (1981). An enhancement and modification of the emission of dye molecules and trivalent rare-earth ions adsorbed onto rough metallic surfaces, metallic islands, engineered structures, etc. have been studied more recently (Weitz et al., 1983; Denisenko et al., 1996; Kikteva et al., 1999; Selvan et al., 1999; Lakowicz et al., 2001). An increase of optical absorption of CdS quantum dots by gold nanospheres has been demonstrated by Biteen et al. (2004).

If a mixture of dye solution and metallic nanoparticles is used as a laser medium, then the SP-induced enhancement of absorption and emission of dye can significantly improve the laser performance. Thus, according to the studies by Kim et al. (1999) and Drachev et al. (2002), in a mixture of rhodamine 6G (R6G) dye with aggregated silver nanoparticles placed in an *optical micro-cavity* (glass capillary tube), local electromagnetic fields are enhanced by many orders of magnitude, and the laser action can be obtained at the pumping power, which is not enough to reach the lasing threshold in a pure dye solution of the same concentration. The experiments in the studies by Kim et al. (1999) and Drachev et al. (2002) were not highly reproducible and the mechanisms of the dramatic reduction of the lasing threshold were not clearly understood. This motivated us to carry out a more systematic study of an analogous system, investigating separately the effects of spontaneous emission, the stimulated emission in a pump-probe setup, and the laser emission in an easy-to-tune two-mirror laser cavity (see Sections 4.2, 4.5, and 4.6).

Most of the existing and potential future applications of nanoplasmonics suffer from damping caused by metal absorption and radiation losses. Over the years, several proposals have been made on how to conquer the plasmon loss. Thus, in 1989 Sudarkin and Demkovich suggested to increase the propagation length of SPP by creating the population inversion in the dielectric medium adjacent to the metallic film (Sudarkin and Demkovich, 1989). The proposed experimental test was based on the observation of increased reflectivity of a metallic film in the frustrated total internal reflection setup. Sudarkin and Demkovich (1989) also briefly discussed the possibility of creating a SP-based laser. This work was preceded by the observation of super-luminescence and light generation by a dye solution under the condition of internal reflection (Kogan

et al., 1972) and the study of gain-enhanced total internal reflection in the presence of metallic film through the mediation of SPPs on the metal surface (Plotz et al., 1979).

The ideas above have been further developed in more recent years. Thus, gain-assisted propagation of SPPs in planar metal waveguides of different geometries has been studied by Nezhad et al. (2004). SPPs at the interface between metal and a dielectric with strong optical gain have been analyzed theoretically by Avrutsky (2004). In particular, it has been shown (Avrutsky, 2004) that the proper choice of optical indices of the metal and dielectric can result in an infinitely large effective refractive index of surface waves. Such resonant plasmons have extremely low group velocity and are localized in a very close vicinity to the interface. The amplification of SPPs at the interface between silver film and dielectric medium with optical gain (laser dye) has been recently demonstrated by Seidel et al. (2005). The observation was done in an experimental setup similar to that proposed by Sudarkin and Demkovich (1989) and the experimentally observed change in the metal reflection was as small as 0.001%.

In a similar way, Lawandy (2004) has predicted the *localized* SP resonance in metallic nanospheres to exhibit a singularity when the surrounding dielectric medium has a critical value of optical gain. This singularity, resulting from canceling *both real* and *imaginary* terms in the denominator of the field enhancement factor in metal nanospheres $\propto (\varepsilon_d - \varepsilon_m)/(2\,\varepsilon_d + \varepsilon_m)$ can be evidenced by an increase of the Rayleigh scattering within the plasmon band and lead to low-threshold random laser action, light localization effects, and enhancement of SERS (Lawandy, 2004) (here ε_d and ε_m are complex dielectric constants of dielectric and metal, respectively).

This study was continued in the work by Lawandy (2005), where a three-component system consisting of (i) metallic nanoparticle, (ii) shell of adsorbed molecules with optical gain, and (iii) surrounding dielectric (solvent) has been considered. In particular, it has been shown that depending on the thickness of the layer of an amplifying shell, the absorption of the complex can be increased or decreased with the increase of the gain in the dye shell (Lawandy, 2005).

A seemingly similar phenomenon has been described in an earlier publication (Bergman and Stockman, 2003) using a completely different set of arguments. Thus, Bergman and Stockman (2003) have proposed a new way to excite localized fields in nanosystems using SP amplification by stimulated emission of radiation (SPASER). SPASER radiation consists of SPs (bosons), which undergo stimulated emission, but, in contrast to

photons, can be localized on the nanoscale. SPASER consists of an active medium with population inversion that transfers its excitation energy by radiationless transitions to a resonant nanosystem, which plays a role analogous to the laser cavity (Bergman and Stockman, 2003; Stockman, 2005). Alternatively, the major features of SPASER can be probably described in terms of Förster dipole–dipole energy transfer (Förster, 1948; Dexter et al., 1969) from an excited molecule (ion, quantum dot, etc.) to a resonant SP oscillation in a metallic nanostructure.

In this chapter, we discuss the demonstrated (i) enhancement of localized SP oscillation in the aggregate of Ag nanoparticles by optical gain in the surrounding dye and (ii) enhancement of spontaneous and stimulated emission of rhodamine 6G (R6G) laser dye by Ag aggregate. The results presented in this chapter have been published in Refs. (Noginov et al., 2005a; Noginov et al. 2006a, b, c).

§ 2. Estimation of the critical gain

Let us estimate a critical gain needed to compensate metal loss of localized SPs. The polarizability (per unit volume) for isolated metallic nanoparticles is given by $\beta = (4\pi)^{-1}[\varepsilon_m - \varepsilon_d] / [\varepsilon_d + p(\varepsilon_m - \varepsilon_d)]$, where p is the depolarization factor (Shalaev, 2000). If the dielectric is an active medium with $\varepsilon_d'' = -p\varepsilon_m''/(1-p)$, then at the resonance wavelength λ_0 both the real and imaginary parts in the denominator become zero, leading to extremely large local fields limited only by saturation effects (Drachev et al., 2004; Lawandy, 2004). Thus, for the gain coefficient needed to compensate loss of *localized* SP, we find $\gamma = (2\pi/\lambda_0)\varepsilon_d''/\sqrt{\varepsilon_d'} = (2\pi/\lambda_0)[p/(1-p)]\varepsilon_m''/n = (2\pi/n\lambda_0)(\Gamma/\omega_p)[p/(1-p)][\varepsilon_b + n^2(1-p)/p]^{3/2} \sim 10^3 \text{cm}^{-1}$ at $\lambda_0 = 0.56\,\mu\text{m}$ (we used the Drude formula $\varepsilon_m = \varepsilon_b - \omega_p^2[\omega(\omega + i\Gamma)]$, $n = 1.33$, $\varepsilon_d = 1.77$, and known optical constants from Johnson and Christy (1972)). The value of the critical gain above is close to that estimated in Ref. (Lawandy, 2005).

The gain $\gamma \sim 10^3$ cm^{-1} needed to compensate loss of SPP or localized SP is within the limits of semiconducting polymers (Hide et al., 1997) or laser dyes (highly concentrated, $\sim 10^{-2}$ M (Lawandy, 2005), or adsorbed onto metallic nanoparticles). One can estimate that a single excited molecule of R6G characterized by the cross section $\sim 4 \times 10^{-16}$ cm^2 adsorbed onto metallic nanoparticle with the diameter d = 10 nm causes the gain coefficient (per the volume occupied by the nanoparticle) of the order of 10^3 cm^{-1}. If the number of adsorbed R6G molecules per nanoparticle exceeds one, the effective gain can be even higher.

§ 3. Experimental samples and setups

Experimentally, we studied mixtures of R6G dye (Rhodamine 590 Chloride from Exciton) and aggregated Ag nanoparticles. The starting solutions of R6G in methanol had concentrations of dye molecules in the range 1×10^{-6} to 2.1×10^{-4} M. Poly(vinylpyrrolidone) (PVP)-passivated silver aggregate was prepared according to the procedure described by Noginov et al. (2005b). The estimated concentration of Ag nanoparticles in the aggregate was 8.8×10^{13} cm^{-3}. In many measurements, Ag was diluted severalfold with methanol before mixing it with the dye.

Absorption spectra of dye solutions, Ag aggregate solutions, and dye–Ag aggregate mixtures were recorded with the UV-VIZ-IR Lambda 900 spectrophotometer (Perkin Elmer). In the emission measurements, the mixtures of R6G dye and Ag aggregate were excited with the frequency-doubled radiation of Q-switched Nd:YAG laser (Quanta Ray, $\lambda = 532$ nm, $t_{\text{pulse}} = 10$ ns, repetition rate 10 Hz). The same pumping was used in the pump-probe gain measurements, the laser experiment, and the pump-probe Rayleigh scattering experiment. The emission spectra were recorded using an MS257 monochromator (Oriel), a photomultiplier tube, and a boxcar integrator. A cw 594 nm He-Ne laser beam was used as a probe in the gain measurements.

In the luminescence kinetics studies, the emission of pure R6G dye solutions and dye–Ag aggregate mixtures was excited with an optical parametric amplifier Topaz (Quantronics/Light Conversion $\lambda = 530$ nm, $t_{\text{pulse}} = 2.5$ ps) pumped with the Spitfire laser system (Spectra Physics). The signal was detected and recorded using 10 GHz GaAs PIN photodetector model ET-4000 (EOTech, rise time < 35 ps) and 2.5 GHz oscilloscope TDS7254 (Tektronix).

§ 4. Experimental results and discussion

4.1. Absorption spectra

The absorption spectrum of Ag aggregate has one structureless band covering the whole visible range and extending to near-infrared (fig. 2, trace 8). The major feature in the absorption spectrum of R6G is the band peaking at ≈ 528 nm (fig. 2a, trace 1 and inset of fig. 2a). The absorption spectra of the mixtures were recorded when Ag aggregate solution was added to the dye solution by small amounts (fig. 2a, traces 2–7). In different particular experiments, the "step" size varied between 1% and

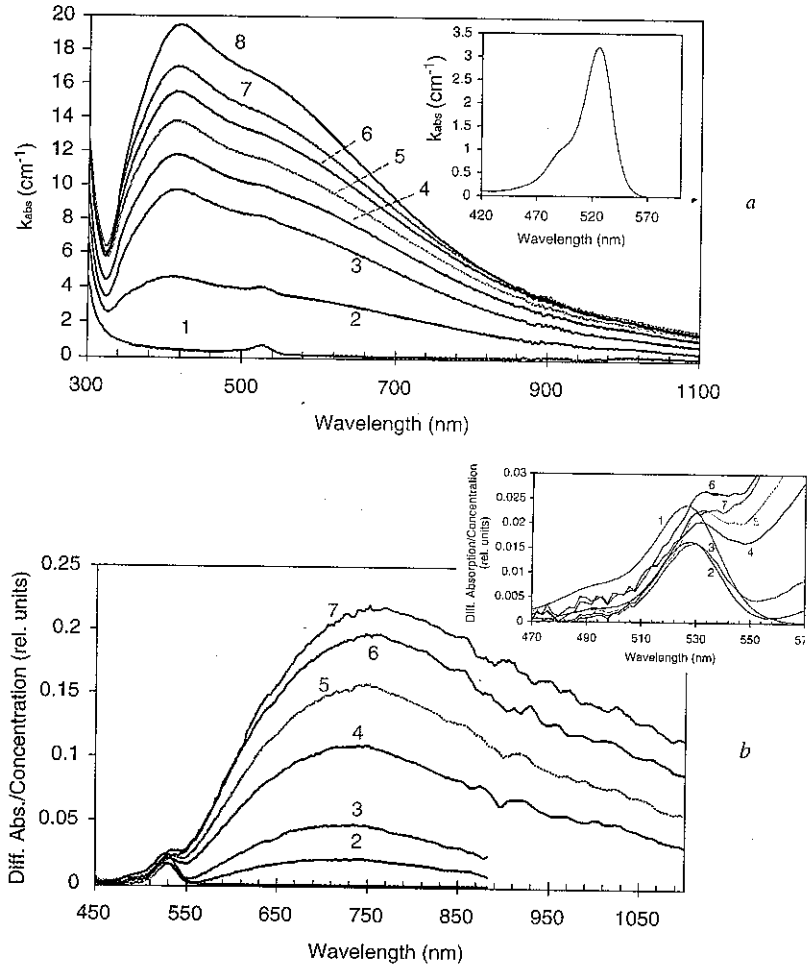

Fig. 2. (a) Trace 1 – Absorption spectrum of pure R6G dye solution (2.1×10^{-6} M); trace 8 – absorption spectrum of pure Ag aggregate solution (8.8×10^{13} cm^{-3}); traces 2–7 – absorption spectra of R6G–Ag aggregate mixtures. The ratio of Ag aggregate solution to R6G solution in the mixture is equal to 27.1/72.9 (2), 57.3/42.7 (3), 66.5/33.5 (4), 74.8/25.2 (5), 80.8/19.2 (6), and 86.8/13.2 (7). Inset: Absorption spectrum of pure R6G dye solution (1.25×10^{-5} M). (b) Difference absorption spectra (absorption spectrum of the mixture minus scaled spectrum of the aggregate, normalized to the concentration of R6G dye in the mixture). The traces in figure b correspond to the spectra with similar numbers in figure a. Inset: Enlarged fragment of the main frame. Trace 1 corresponds to pure R6G dye.

25% of the maximal Ag concentration. We then scaled the absorption spectrum of pure Ag aggregate to fit each of the spectra of the mixtures at $\leqslant$450 nm and calculated the differential spectra (*mixture–aggregate*). The differential spectra obtained this way, normalized to the concentration of the R6G dye in the mixture, reveal the regular absorption band of R6G dye, at ~0.53 μm, and a much broader new absorption band centered at 0.72–0.75 μm (fig. 2b). The latter broad band can be due to hybrid states formed by R6G molecules chemisorbed (via Cl^-) onto silver nanoparticles (Fang, 1999) or due to restructuring of the Ag aggregate in the presence of dye molecules.

With the increase of Ag aggregate concentration in the mixture, the intensity of the absorption band of R6G (calculated using the procedure described above) decreased, with the rate exceeding the reduction of the R6G concentration (fig. 2b). This reduction will be discussed in detail in Section 4.4. (The observed reduction of the R6G absorption is due to Ag aggregate but not an aggregate solvent without Ag (Noginov et al., 2005c)). The slight spectral shift of the R6G absorption band (from 528 to 531 nm) with the increase of the Ag aggregate concentration can be partially explained by its "mechanical" overlap with the strong absorption band peaking at 0.72–0.75 μm.

4.2. *Spontaneous emission*

Spontaneous emission spectra of the dye–Ag aggregate mixtures were studied in the setup schematically shown in the low left corner inset of fig. 3, when the dye or a mixture of dye with Ag aggregate was placed in a 1 mm thick cuvette. The samples were pumped and the luminescence was collected nearly normally to the surface of the cuvette. We found that while the shape of the emission band (upper right corner inset of fig. 3) was practically unaffected by the presence of Ag aggregate in the mixture, its intensity changed significantly. At the starting concentrations of R6G and Ag aggregate, equal to R6G = 1.25×10^{-5} M, Ag = 8.7×10^{12} cm^{-3}, the emission intensity of the dye (measured in the maximum at ~558 nm) increased up to 45% with the addition of small amounts of aggregated silver nanoparticles (fig. 3). At the further increase of the concentration of Ag aggregate in the mixture, the emission intensity decreased. This reduction was, in part, due to the absorption by Ag aggregate of both pumping and emission. Another possible reason for the reduction of the emission intensity was quenching of dye luminescence by silver nanoparticles. However, the relative decrease of the emission intensity was

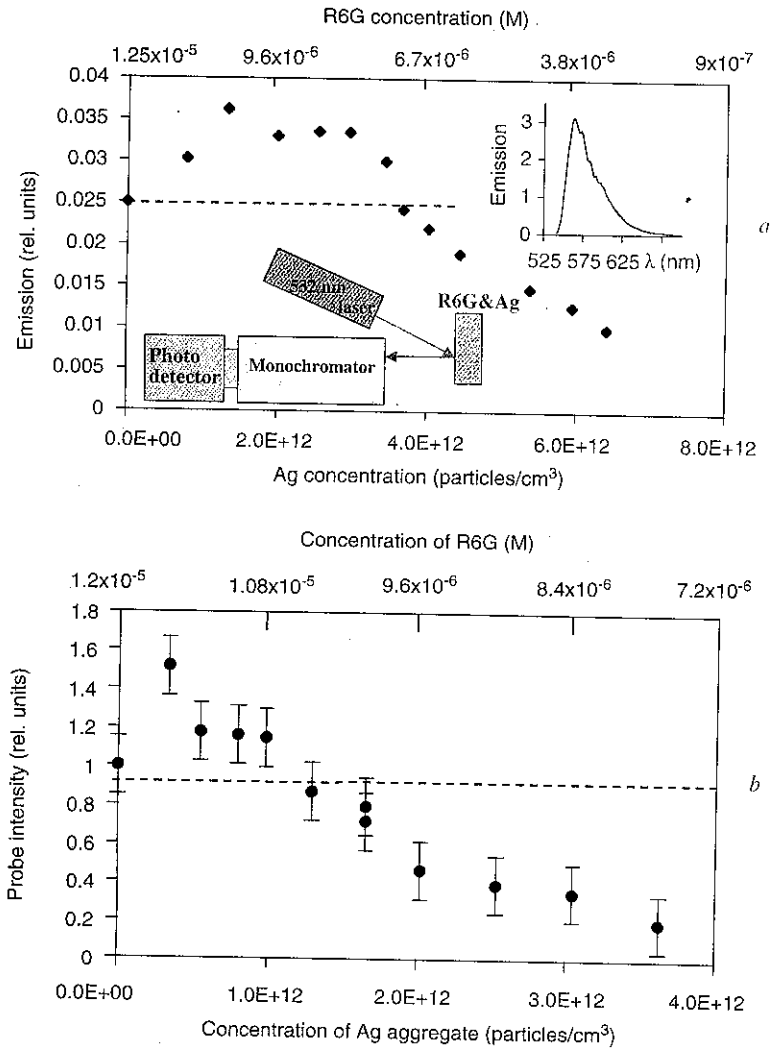

Fig. 3. (a) Emission intensity recorded at the addition of Ag aggregate to R6G dye. The starting concentrations of R6G and Ag aggregate are, respectively, 1.25×10^{-5} M and 8.7×10^{12} cm^{-3} The emission intensity corresponds to "as is" detected signal that has not been a subject to any normalization. Inset in the low left corner: Schematic of the experimental setup used at the emission intensity measurement. Inset in the upper right corner: Emission spectrum of R6G dye. (b) Probe light intensity (at $\lambda = 594$ nm) measured in a pump-probe gain experiment in 10 mm cuvette at the 532 nm pumping energy equal to 0.38 mJ (after 0.5 mm pinhole) as a function of the R6G and Ag aggregate concentrations. All detected signals are normalized to that in pure dye solution.

much smaller than the relative reduction of the R6G absorption determined according to the procedure described above.

At low concentrations, i.e., $\leqslant 2.1 \times 10^{-5}$ M, of R6G used in the majority of our experiments, the spontaneous emission kinetics recorded in pure dye solutions was nearly single exponential. The measured time constant was ~25% larger than the 3.6–3.8 ns lifetime of R6G known from the literature (Selanger et al., 1977; Müller et al., 1996; Zander et al., 1996). The elongation of the decay kinetics was probably due to the reabsorption, which could not be completely neglected, since at certain emission wavelengths (~550 nm) the absorption length of dye was comparable to the linear size of the cuvette (~1 cm). When dye ($< 2 \times 10^{-5}$ M) was mixed with Ag aggregate ($< 1.3 \times 10^{13}$ cm^{-3}), the effective emission decay time shortened to ~88% of its maximal value in pure dye (fig. 4). (We assume that the reabsorption was weak enough to affect the qualitative character of the dependence in fig. 4 significantly.) One can hypothesize that dye molecules, which luminescence decay-times are shortened by the presence of Ag aggregate, are situated close to metallic nanoparticles and their absorption and emission properties are affected by SP-enhanced fields.

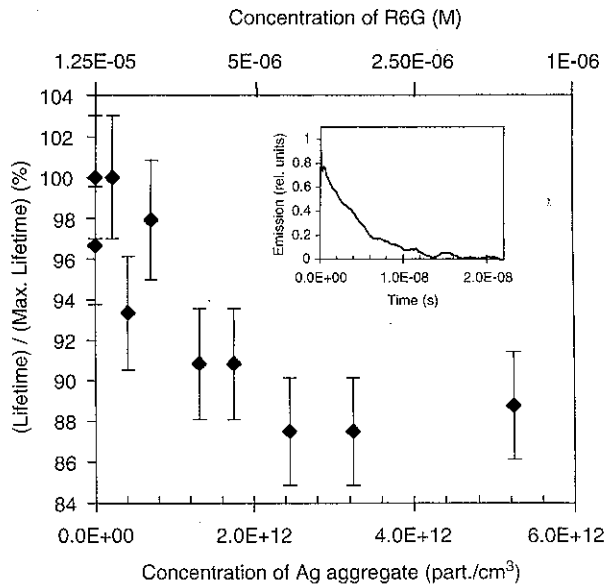

Fig. 4. Dependence of the R6G emission lifetime on concentration of Ag aggregate in dye–Ag aggregate mixtures characterized by low concentrations of R6G dye. All values are normalized to the lifetime measured in the pure R6G solution. Inset: Typical emission kinetics.

4.3. Enhanced Rayleigh scattering due to compensation of loss in metal by gain in dielectric

Following the prediction by Lawandy (2004), we sought for the enhancement of Rayleigh scattering by silver nanoparticles embedded in the dye with optical gain. In the pump-probe experiment, a fraction of the pumping beam was split off and used to pump a laser consisting of the cuvette with R6G dye placed between two mirrors (inset of fig. 5a). The emission line of the R6G laser (~558 nm) corresponded to the maximum of the gain spectrum of R6G dye in the mixtures studied. The beam of the R6G laser, which was used as a probe in the Rayleigh scattering, was aligned with the pumping beam in the beamsplitter and sent to the sample through a small (0.5 mm) pinhole (inset of fig. 5a). The pump and probe beams were collinear, and their diameters at the pinhole were larger than 0.5 mm.

The scattered light was collected by an optical fiber that was placed within several millimeters from the cuvette at the angles ranging from ~45° to ~135° relative to the direction of the beam propagation. (We did not notice that the results of the SP enhancement measurement depended on the detection angle.) The fiber collected scattered *probe* light as well as scattered *pumping* light and spontaneous emission of dye. To separate the scattered probe light, we used a monochromator and ran the emission spectrum from 540 to 650 nm.The scattered probe light was seen in the spectrum as a relatively narrow (~5 nm) line on the top of a much broader spontaneous emission band.

Experimentally, we kept the energy of the probe light constant and measured the intensity of the scattered probe light as the function of the varied pumping light energy. The sixfold increase of the Rayleigh scattering observed in the dye–Ag aggregate mixture with the increase of the pumping energy (fig. 5a, squares) is the clear experimental demonstration of the compensation of loss in metal and the enhancement of the quality factor of SP resonance by optical gain in surrounding dielectric.

The dye–Ag aggregate mixtures were placed in 1 mm thick cuvettes. At the dye concentration, 2.1×10^{-5} M, which we used in the majority of our experiments, the maximal optical amplification (of the pure dye solution or dye–Ag aggregate mixtures) at 1 mm length did not exceed ~7% (see Section 4.5). The lateral dimension of the pumped volume was smaller than 1 mm.The dye–Ag aggregate mixtures were visually clear, with the transport mean free path of the order of centimeters. Correspondingly, the probability of elongation of photon path in the *pumped* volume due to

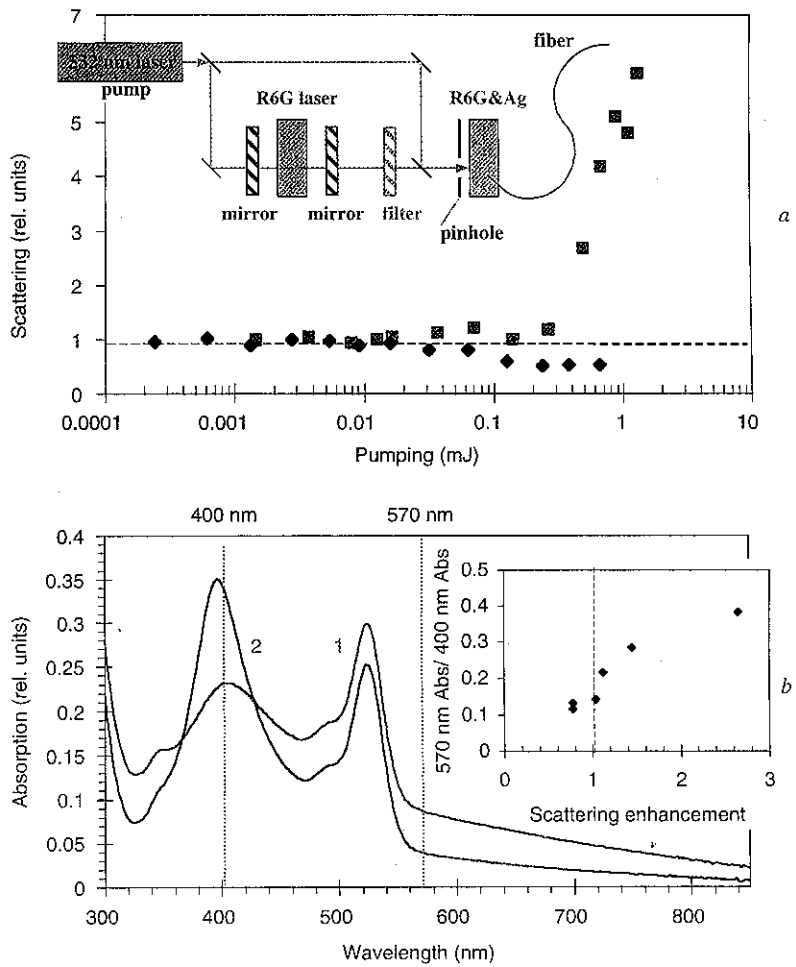

Fig. 5. (a) Intensity of the Rayleigh scattering as the function of the pumping energy. (b) Absorption spectra of the dye–Ag aggregate mixtures; R6G – 2.1×10^{-5} M, Ag aggregate – 8.7×10^{13} cm^{-3}. Squares in (a) and trace 1 in (b) correspond to one mixture, and diamonds in (a) and trace 2 in (b) correspond to another mixture. Inset of (a): Pump-probe experimental setup for the Rayleigh scattering measurements. Inset of (b): The ratio of the absorption coefficients of the dye–Ag aggregate mixtures at 570 and 400 nm plotted vs. the enhancement of the Rayleigh scattering measured at 0.46 mJ.

scattering was insignificantly small. Thus, we conclude that an increase of the intensity of scattered light in our experiment was due to an enhancement of the Rayleigh scattering cross section of metallic particles rather than a simple amplification of scattered light in a medium with gain.

(Note that low average gain in the volume of the cuvette is not inconsistent with the existence of high local gain in vicinity of silver nanoparticles caused by adsorbed molecules). Experimentally, no noticeable enhancement of scattering was observed in the pure R6G dye solution or pure Ag aggregate suspension.

Depending on the shape of the absorption spectrum of the Ag aggregate–dye mixture (fig. 5b), the intensity of the Rayleigh scattering could increase or decrease with the increase of pumping (fig. 5a). Inset of fig. 5b shows a monotonic dependence of the scattering enhancement measured at 0.46 mJ pumping energy vs. the ratio of the absorption coefficients of the mixture at 570 and 400 nm. One can see that the relatively strong absorption of the mixture at 570 nm, which is a signature of *aggregated* Ag nanoparticles, helps to observe an enhanced Rayleigh scattering. Although we do not precisely understand the relationship between the absorption spectra and the physical properties of the mixtures, which govern the results of the scattering experiments, the correlation exists with no doubts.

A plausible explanation for different scattering properties of different mixtures could be in line with the theoretical model developed by Lawandy (2005), in which a three-component system consisting of metallic nanoparticle, shell of adsorbed molecules with optical gain, and surrounding dielectric (solvent) has been studied. In particular, it has been shown that depending on the thickness of the layer of an amplifying shell, the absorption of the complex can be increased or decreased with the increase of the gain in dye (Lawandy, 2005). Similarly, we can speculate that in our experiments, in different mixtures we had different numbers of adsorbed molecules per metallic nanoparticle, which determined the enhancement or the reduction of the Rayleigh scattering.

4.4. Discussion of the results of the absorption and emission measurements

4.4.1. Suppression of the SP resonance by absorption in surrounding dielectric media

Using the same line of arguments as was used by Lawandy (2004), one can infer that by embedding metallic nanoparticle in a dielectric medium with *absorption*, one can further increase the imaginary part of the denominator in the field enhancement factor $\propto [\varepsilon_m - \varepsilon_b]/[\varepsilon_d + p(\varepsilon_m - \varepsilon_d)]$ and, correspondingly, reduce the quality factor of the plasmon resonance and the peak absorption cross section. This effect should always

accompany the effect of the SP enhancement by gain and be observed in the same dye–Ag aggregate mixtures. The absorption coefficient of the dielectric medium, which is comparable to the critical value of gain $\sim 10^3$ cm^{-1}, should be adequate for the observation of a significant damping of a SP resonance.

4.4.2. Emission intensity and absorption

What is the reason for the increase of the spontaneous emission intensity with the addition of Ag aggregate to the R6G dye solution? The quantum yield of spontaneous emission of low-concentrated R6G dye is ~95% (Kubin and Fletcher, 1982; Magde et al., 2002); thus, the experimentally observed emission enhancement cannot be due to the increase of the quantum yield. An enhancement of emission can be explained by increased absorption of R6G in the presence of Ag aggregate. However, at the first glance, this explanation contradicts with the experimental observation: seeming reduction of the R6G absorption with the increase of Ag aggregate concentration (inset of fig. 2b).

We argue that the commonly accepted procedure of the decomposition of an absorption spectrum into its components, which we used to treat data of fig. 2, is not applicable to the mixture of two substances (dye and aggregated Ag nanoparticles), which affect each other, and that the paradox above has a clear physical explanation.

The absorption spectrum of a fractal aggregate is comprised of a continuum of homogeneous bands corresponding to metallic nanostructures with different effective form factors. The homogeneous widths of individual bands are comparable to the characteristic widths of the absorption and emission bands of R6G dye. Following our prediction of the suppression of the SP resonance by the absorption in a dielectric, we speculate that the absorption band of R6G "burns" a hole in the absorption spectrum of the aggregate in the frequency range corresponding to the absorption of dye. Thus, the conventional method that we used to extract the absorption band of R6G from the absorption spectrum of the mixture was not applicable to our system. Instead, the absorption spectrum of the mixture should be decomposed according to the method schematically shown in fig. 6. This explanation suggests that we have experimentally observed the predicted suppression of the SP resonance by absorption in the surrounding dielectric medium. The experimental observation of this effect provides additional support to our claim above of the enhancement of the SP by gain.

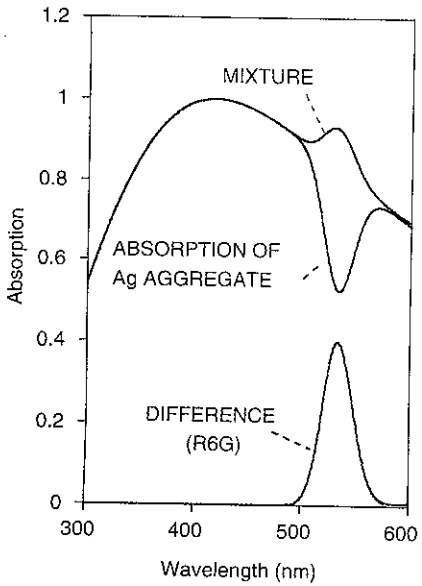

Fig. 6. Schematic of the proposed decomposition of the absorption spectrum of the mixture into the absorption spectra of the components.

4.5. *Stimulated emission studied in a pump-probe experiment*

The enhancement of stimulated emission of R6G dye by Ag aggregate was studied in a pump-probe experiment, which scheme is shown in inset of fig. 7a. The mixture of R6G dye and silver nanoparticles (placed in 10 mm cuvette) was pumped with ~10 ns pulses of a frequency-doubled Nd-YAG laser (532 nm) and probed with a cw 594 nm He-Ne laser. The two beams were collinear. They were centered at 0.5 mm pinhole that was attached to the front wall of the cuvette and restricted the diameters of the incoming beams. The amplification of the probe light (during the short pumping pulse) was measured using 1 GHz oscilloscope TDX 784D (Tektronix). To minimize the amount of spontaneous emission light reaching the detector, we used a monochromator, which wavelength was set at 594 nm.To subtract the residual luminescence signal from the amplified probe light, we repeated the same measurements two times, with and without the probe light.

The result of the measurements for a pure R6G dye solution (1.25×10^{-5} M) is depicted in fig. 7 (diamonds). The dependence of the amplification of the probe light (defined as the ratio of the output and input

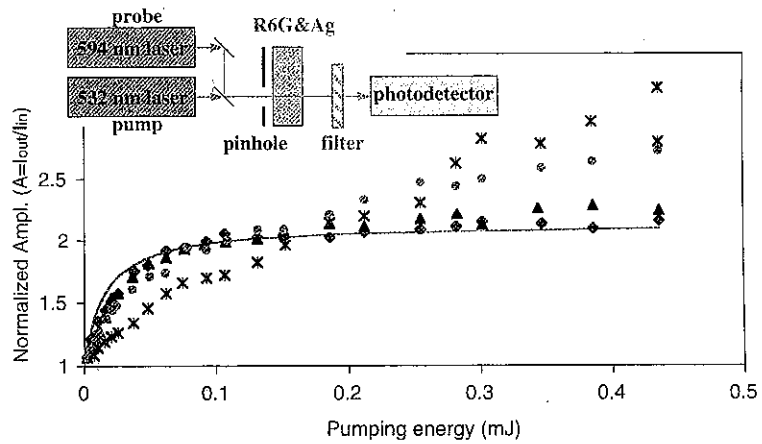

Fig. 7. Amplification $A = I_{out}/I_{in}$ (at $\lambda = 594$ nm) as a function of the 532 nm pumping energy (after 0.5 mm pinhole) measured in a series of R6G dye–Ag aggregate solutions in 10 mm cuvette. Solid line – calculation corresponding to pure dye, 1.25×10^{-5} M. Characters – experiment. Diamonds – pure dye, 1.25×10^{-5} M; triangles – dye, 1.25×10^{-5} M, Ag aggregate, 3.6×10^{11} particles/cm^3; circles – dye, 9.0×10^{-6} M, Ag aggregate, 2.5×10^{12} particles/cm^3; crosses – dye, 5.1×10^{-6} M, Ag aggregate, 5.2×10^{12} particles/cm^3. All amplification signals are normalized to the transmission in corresponding not pumped media. Inset: schematic of the experiment.

probe light intensities I_{out}/I_{in}, on the pumping power density $P(t)/S$) was described in terms of equations

$$0 \approx \frac{dn^*}{dt} = \frac{P(t)}{Shv_p}\sigma^{dye}_{abs\ 532}(N - n^*) - \frac{n^*}{\tau} \quad \text{and} \tag{4.1}$$

$$A \equiv \frac{I_{out}}{I_{in}} = \exp(n^*\sigma^{dye}_{em\ 594}l) \tag{4.2}$$

where n^* is the population of the metastable excited state of R6G; N is the concentration of R6G molecules in the solution; hv_p is the energy of the pumping photon; τ is the spontaneous emission lifetime; $\sigma^{dye}_{em\ 594}$ is the emission cross section of R6G at the probe wavelength (Svelto, 1998); $\sigma^{dye}_{abs\ 532}$ is the absorption cross section of R6G at the pumping wavelength; and l is the length of the cuvette. In the model, we assumed a four-level scheme of R6G (Svelto, 1998), with the pumping transition terminating at a short-lived state above the metastable state. Thus, we neglected any stimulated emission at the *pumping* wavelength. Since the duration of the pumping pulse was twice longer than the luminescence decay time, we assumed a quasi-cw regime of pumping ($dn^*/dt \approx 0$).

A good qualitative and quantitative agreement between the calculation (solid line in fig. 7) and the experiment (diamonds) confirms the adequacy of the model. The saturation in the system occurs when all dye molecules are excited and stronger pumping cannot cause a larger gain.

When Ag aggregate was added to the mixture, it caused absorption at the wavelength of the probe light. Correspondingly, in order to obtain the true value of A, all measured amplification signals in the dye–Ag aggregate mixtures were normalized to the transmission T of the probe light through the not pumped sample. The transmission of the sample was checked before and after each amplification measurement. In addition, the solution was thoroughly stirred before measuring each new data point. This helped us to minimize the possible effect of the photomodification of the mixture on the measurement results. The analysis of the probe signal kinetics revealed the existence of at least two different photoinduced lenses, both having characteristic times longer that the duration of the pumping pulse, ~10 ns. Those photoinduced lenses did not interfere with the observation significantly, and the study of their nature was outside the scope of this work.

The results of the amplification measurements in the mixed samples are summarized in fig. 7. The most remarkable feature of this experiment is that in the presence of Ag aggregate, the value of the amplification is not limited by the saturation level characteristic of pure dye but grows to larger magnitudes. Since at strong pumping ($\geqslant$2 mJ) all dye molecules are already excited, the observed enhancement of the amplification cannot be due to the increased absorption efficiency. We speculate that it is rather due to the enhancement of the *stimulated emission* efficiency caused by the field enhancement in the vicinity of aggregated Ag nanoparticles. Note that the enhancement of *stimulated emission* and the enhancement of *absorption* are caused by the same physical mechanisms and are expected to accompany each other.

When we added Ag aggregate to the mixture, we diluted R6G dye. The dilution of dye, on its own, should lead to the reduction of the gain saturation level. Partial absorption of pumping by Ag aggregate should also lead to the reduction of the amplification. These two factors make the result presented in fig. 7 (enhancement of amplification) even more remarkable.

An increase of the *spontaneous* emission intensity with the addition of Ag aggregate to the mixture is shown in fig. 3a. In approximately the same range of the R6G and Ag aggregate concentrations and at very small pumping energies ($\leqslant$0.4 mJ), we have observed an *absolute* enhancement of the probe light amplification, without any renormalization

to the sample transmission (fig. 3b). The observed increase of the amplified signal could be due to the combination of enhancements of stimulated emission and absorption.

It appears likely that the interplay between the enhancements of absorption and emission, which increase an amplified signal, and the dilution of dye as well as an absorption dye to Ag aggregate, which reduce amplification, may cause a complex behavior of the system, which is critically dependent on the Ag concentration and pumping intensity.

4.6. *Effect of Ag aggregate on the operation of R6G dye laser*

In this particular experiment, we studied the effect of Ag aggregate on the performance of R6G dye laser. We expected to reduce the lasing threshold by adding Ag aggregate to the dye solution, as it was demonstrated by (Kim et al., 1999; Drachev et al., 2002), where a glass capillary resonator was used.

The easy-to-tune laser setup consisted of the rear dichroic mirror, through which the gain element (10 mm cuvette with dye or dye–Ag aggregate mixture) was pumped, and the output mirror (fig. 8a). All mirrors were flat. The back mirror had the reflectivity coefficient $R = 99.96\%$ (at the stimulated emission wavelength $\lambda \sim 558$ nm). Several output mirrors, which we used, had reflectivities R equal, respectively, to 99.7%, 87.8%, 46.0%, and 17.5%. The distance between the mirrors was 6.8 cm, and the cuvette with the gain medium was positioned approximately in the center of the cavity. The lens with the focal length equal to 18 cm focused pumping light (Q-switched 532 nm laser radiation) into approximately 0.5 mm spot in the cuvette. The color filter placed after the output mirror helped to separate the laser emission from the residual pumping leaking through the laser cavity.

With the addition of the Ag aggregate to the R6G dye solution, instead of anticipated enhancement of the laser output, we observed an increase of the lasing threshold and a reduction of the slope efficiency. The representative series of input–output curves is shown in fig. 8b. Apparently, at the sets of the parameters, which were used in our experiments, the reduction of the stimulated emission output caused by the dilution of dye and the addition of a gray absorbing substance (Ag aggregate) to the laser cavity overcame the increase of the stimulated emission intensity caused by the SP field enhancement in metallic nanostructures.

In order to evaluate the positive impact of the SP field enhancement on laser operation, we compared the experimental laser thresholds measured

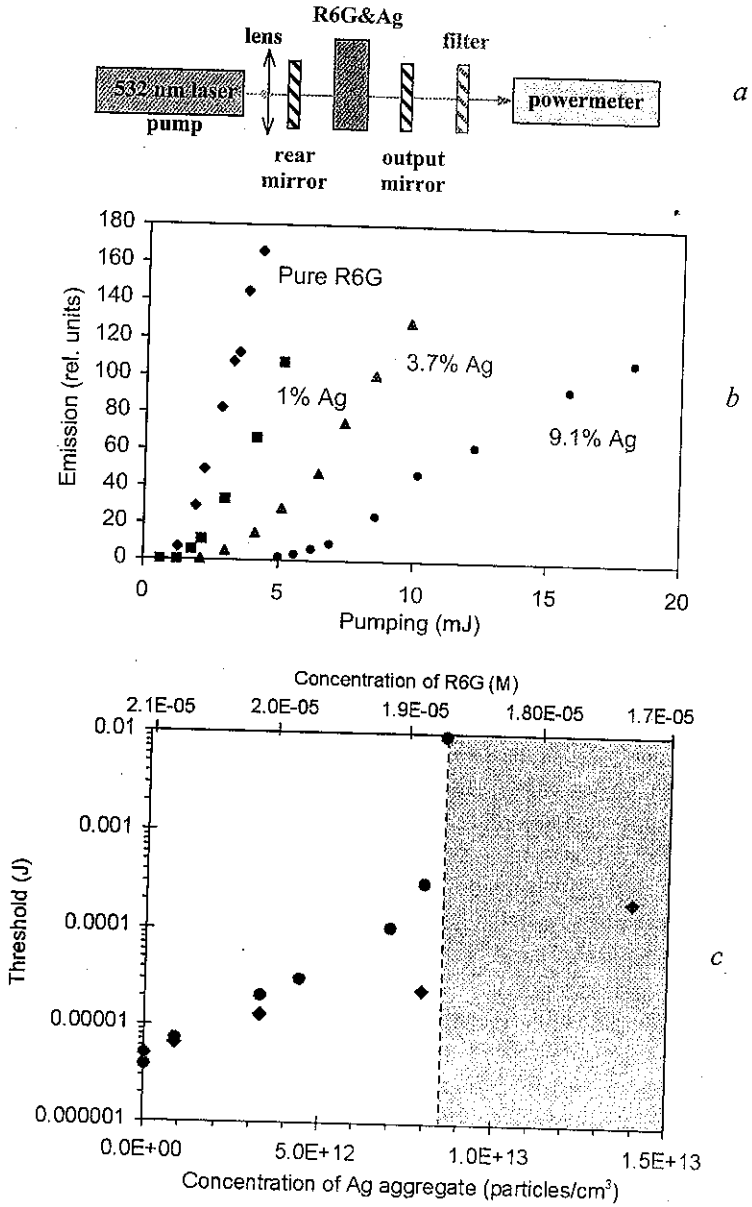

Fig. 8. (a) Laser setup; (b) the input–output laser curves (at $\lambda \sim 560$ nm) recorded in a series of samples prepared by mixing small amounts of Ag aggregate (8.8×10^{12} particles/cm^3) with R6G dye (1.1×10^{-5} M). The volume percentage of the Ag aggregate is indicated next to each curve. (c) Experimental (diamonds) and calculated (circles) dependences of the laser threshold on Ag aggregate concentration. $R_{out} = 99.7\%$, $L = 15.6\%$.

in a series of dye–aggregate mixtures with the thresholds calculated under the assumption that the only two effects of the aggregate were (i) the dilution of dye and (ii) an increase of parasitic absorption at the pumping and emission wavelengths. We first evaluated the threshold population inversion n_{th} [cm^{-3}], which is required to conquer loss at the lasing wavelength, and then calculated the value of the incident pumping energy E_{th} [J], which is needed to create this population inversion.

Thus, the value n_{th} was calculated from the formula equating the gain and the loss at the lasing threshold

$$\exp(2l\sigma^{dye}_{em\ 560}n_{th})\exp\{-2l[(k^{dye}_{abs\ 560} - \sigma^{dye}_{abs\ 560}n_{th}) + k^{Ag}_{abs\ 560}]\} \times R_1R_2(1-L) = 1, \tag{4.3}$$

and the value E_{th} was calculated from the formula for the threshold rate of the pumping absorption per unit volume F_{th} [cm^{-3}s^{-1}]

$$F_{th} = \frac{E_{th}}{t_p h\nu_p (Sl)}\{1 - \exp[-((k^{dye}_{abs\ 532} - n_{th}\sigma^{dye}_{abs\ 532}) + k^{Ag}_{abs\ 532})l]\} \left\{\frac{(k^{dye}_{abs\ 532} - n_{th}\sigma^{dye}_{abs\ 532})}{[(k^{dye}_{abs\ 532} - n_{th}\sigma^{dye}_{abs\ 532}) + k^{Ag}_{abs\ 532}]}\right\}, \tag{4.4}$$

which, in turn (in quasi-cw approximation), is related to n_{th} as

$$F_{th} = \frac{n_{th}}{\tau}. \tag{4.5}$$

Here l is the length of the laser element, $\sigma^{dye}_{abs(em)xxx}$ is the absorption (emission) cross section of dye at the wavelength λ (nm), $k^{dye(Ag)}_{abs\ xxx}$ is the absorption coefficient of dye (Ag aggregate) at the concentration corresponding to the particular mixture at λ (nm), R_1 and R_2 are the reflection coefficients of the laser mirrors, L is the parasitic intracavity loss per roundtrip (reflections of the cuvette walls, etc.), t_p is the duration of the pumping pulse, and S is the cross-sectional area of the pumping beam. In eq. (4.4), the first term in figure brackets determines the fraction of incident pumping energy, which is absorbed in the sample, and the second term in figure brackets determines the fraction of the total absorbed pumping energy, which is consumed by *dye* but not by Ag aggregate.

The experimental and the calculated dependences of the laser threshold on the Ag aggregate concentration are depicted in fig. 8c. A good agreement between the experimental and the calculated values of the threshold in the absence of Ag aggregate justifies the accuracy of our model. One can see in fig. 8c that if the enhancements of absorption and stimulated

emission by Ag aggregate are neglected and the role of the aggregate is reduced to the dilution of dye and the increase of the parasitic absorption, the calculated threshold values in dye–Ag aggregate mixtures significantly exceed the experimental ones. On the right hand side of the dashed line in fig. 8c, no lasing is predicted. (In that range of Ag aggregate concentrations, the calculated threshold value of the population inversion n_{th} exceeds the concentration of dye molecules in the solution.) This confirms that Ag aggregate enhances the stimulated emission of R6G dye. However, the overall effect of the aggregate on the laser operation is negative.

How can one make the overall effect of Ag aggregate on the laser output to be positive? As it is shown in Ref. (Noginov et al. 2006c) the improvement of the laser performance at the addition of Ag aggregate to R6G dye should be expected at large values of the output coupling and the value of the threshold population inversion close to the total concentration of dye molecules in the solution. The detailed discussion of the optimal laser parameters is outside the scope of this Chapter.

§ 5. Summary

To summarize, we have observed the compensation of loss in metal by gain in interfacing dielectric in the mixture of aggregated silver nanoparticles and rhodamine 6G laser dye. The demonstrated sixfold enhancement of the Rayleigh scattering is the evidence of the quality factor increase of the SP resonance. This paves the road for numerous applications of nanoplasmonics, which currently suffer from strong damping caused by absorption loss in metal. We have also predicted and experimentally observed the counterpart of the phenomenon above, namely, the suppression of the SP in metallic nanostructure embedded in a dielectric medium with absorption.

We have demonstrated that by adding the solution of aggregated silver nanoparticles to the solution of rhodamine 6G laser dye, one can enhance the efficiency of the spontaneous and the stimulated emission. We attribute an increase of the *spontaneous emission* intensity of dye to the increase of the *absorption* efficiency caused by the field enhancements in metallic nanostructures associated with SPs. The enhancement of the *stimulated emission* of R6G dye, which has the same nature as the enhancement of absorption (SP-induced field enhancement), was observed in the pump-probe and laser experiments. In the dye–Ag aggregate mixtures studied, the positive effect of the stimulated emission enhancement could not overcome in the laser experiment the negative effects associated with the dilution of dye by Ag aggregate and parasitic absorption of Ag aggregate.

Acknowledgments

The work was supported by the following grants: NASA #NCC-3-1035, NSF #HRD-0317722 and DMR-0611430, NSF-NIRT #ECS-0210445, ARO #W911NF-04-1-0350, MURI-ARO 50342-PH-MUR and MURI-ARO 50372-CH-MUR.

References

Averitt, R.D., Westcott, S.L., Halas, N.J., 1999, Linear optical properties of gold nanoshells, J. Opt. Soc. Am. B, **16**, 1824–1832.

Avrutsky, I., 2004, Surface plasmons at nanoscale relief gratings between a metal and a dielectric medium with optical gain, Phys. Rev. B **70**, 155416/1–155416/6.

Bergman, D.J., Stockman, M.I., 2003, Surface plasmon amplification by stimulated emission of radiation: quantum generation of coherent surface plasmons in nanosystems, Phys. Rev. Lett. **90**, 027402/1–027402/4.

Biteen, J., Garcia-Munoz, I., Lewis, N., Atwater, H., 2004, California Institute of Technology, Pasadena, California, MRS Fall Meeting.

Bonod, N., Reinisch, R., Popov, E., Neviere, M., 2004, Optimization of surface-plasmon-enhanced magneto-optical effects, J. Opt. Soc. Am. B **21**, 791–797.

Brongersma, M.L., Hartman, J.W., Atwater, H.A., 2000, Electromagnetic energy transfer and switching in nanoparticle chain arrays below the diffraction limit, Phys. Rev. B **62**, R16356–R16359.

Brus, L.E., Nitzan, A., 1983, Chemical processing using electromagnetic field enhancement", U.S. Patent No.: 4,481,091 (21 October, 1983)., US patent no.: 4,481,091, Chemical processing using electromagnetic field enhancement.

Denisenko, G.A., Malashkevich, G.E., Tziganova, T.V., Galstyan, V.G., Voitovich, A.P., Perchukevich, P.P., Kalosha, I.I., Bazilev, A.G., Mchedlishvili, B.V., Strek, W., Oleinikov, V.A., 1996, Influence of silver surface structure on luminescence characteristics of europium doped polymer films, Acta Physica Polonica A **90**, 121–126.

Dexter, D.L., Förster, Th., Knoh, R.S., 1969, The radiationless transfer of energy of electronic excitation between impurity molecules in crystals, Phys. Stat. Solidi **34**, K159–K162.

Drachev, V.P., Buin, A.K., Nakotte, H., Shalaev, V.M., 2004, Size dependent $\chi(3)$ for conduction electrons in Ag nanoparticles, Nano Lett. **4**, 1535–1539.

Drachev, V.P., Cai, W., Chettiar, U., Yuan, H.-K., Sarychev, A.K., Kildishev, A.V., Shalaev, V.M., 2006, Experimental verification of optical negative-index materials, Laser Phys. Lett. **3**, 49–55/DOI 10.1002/lapl.200510062.

Drachev, V.P., Kim, W.-T., Safonov, V.P., Podolskiy, V.A., Zakovryashin, N.S., Khaliullin, E.N., Shalaev, V.M., Armstrong, R.L., 2002, Low-threshold lasing and broad-band multiphoton-excited light emission from Ag aggregate-adsorbate complexes in microcavity, J. Mod. Opt. **49**, 645–662.

Drachev, V.P., Thoreson, M.D., Khaliullin, E.N., Davisson, V.J., Shalaev, V.M., 2004, Surface-enhanced raman difference between human insulin and insulin lispro detected with adaptive nanostructures, J. Phys. Chem. B **108**, 18046–18052.

Drexhage, K.H., 1974, Interaction of dye with monomolecular dye layers. In: Wolf, E. (Ed.), Progress in Optics XII, New York, North-Holland, 164–232.
Fang, Y., 1999, Acid with visible and near-infrared excitations, J. Raman Spectrosc. **30**, 85–89.
Fang, N., Lee, H., Zhang, X., 2005, Sub-diffraction-limited optical imaging with a silver superlens, Science **308**, 534–537.
Ferrell, T.L., 1994, Thin-foil surface-plasmon modification in scanning-probe microscopy, Phys. Rev. B **50**, 14738–14741.
Fleischmann, M., Hendra, P.J., McQuillan, A.J., 1974, Raman spectra of pyridine adsorbed at a silver electrode, Chem. Phys. Lett. **26**, 163–166.
Förster, Th., 1948, Zwischenmolekulare energiewändler und fluoreszenz, Ann. Phys. **2**, 55–75.
Ghaemi, H.F., Thio, T., Grupp, D.E., Ebbesen, T.W., Lezec, H.J., 1998, Surface plasmons enhance optical transmission through subwavelength holes, Phys. Rev. B **58**, 6779.
Glass, A.M., Liao, P.F., Bergman, J.G., Olson, D.H., 1980, Interaction of metal particles with adsorbed dye molecules: absorption and luminescence, Opt. Lett. **5**, 368–370.
Glass, A.M., Wokaun, A., Heritage, J.P., Bergman, J.P., Liao, P.F., Olson, D.H., 1981, Enhanced two-photon fluorescence of molecules adsorbed on silver particle films, Phys. Rev. B **24**, 4906–4909.
Hayes, C.L., Van Duyne, R.P., 2003, Dichroic optical properties of extended nanostructures fabricated using angle-resolved nanosphere lithography, Nano Lett. **3**, 939–943.
Hide, F., Schwartz, B.J., Díaz-García, M.A., Heeger, A.J., 1997, Conjugated polymers as solid-state laser materials, Synth. Metals **91**, 35–40.
Hutson, L., 2005, Golden eye, Mater, World **13**(6), 18–19.
Johnson, P.B., Christy, R.W., 1972, Optical constants of the noble metals, Phys. Rev. B **6**, 4370–4379.
Kikteva, T., Star, D., Zhao, Z., Baisley, T.L., Leach, G.W., 1999, Molecular orientation, aggregation, and order in Rhodamine films at the fused silica/air interface, J. Phys. Chem. B **103**, 1124–1133.
Kildishev, A.V., Cai, W., Chettiar, U., Yuan, H.-K., Sarychev, A.K., Drachev, V.P. Shalaev, V.M., 2006, Negative refractive index in optics of metal-dielectric composites, JOSA B, will be published in the March issue, 2006.
Kim, W., Safonov, V.P., Shalaev, V.M., Armstrong, R.L., 1999, Fractals in microcavities: giant coupled, multiplicative enhancement of optical resonances, Phys. Rev. Lett. **82**, 4811–4814.
Kneipp, K., Kneipp, H., Itzkan, I., Dasari, R.R., Feld, M.S., 2002, Topical review: surface-enhanced Raman scattering and biophysics, J. Phys. **14**, R597–R624.
Kneipp, K., Wang, Y., Kneipp, H., Perelman, L.T., Itzkan, I., Dasari, R.R., Feld, M.S., 1997, Single molecule detection using surface-enhanced Raman scattering (SERS), Phys. Rev. Lett. **78**, 1667–1670.
Kogan, B.Ya., Volkov, V.M., Lebedev, S.A., 1972, Superluminescence and generation of stimulated radiationunder internal-reflection conditions, JETP Lett. **16**, 100.
Kreibig, U., Vollmer, M., 1995, Optical Properties of Metal Clusters, vol. 25, Springer, New York.
Kubin, R.F., Fletcher, A.N., 1982, Fluorescence quantum yields of some rhodamine dyes, J. Luminescence **27**, 455–462.
Lakowicz, J.R., Gryczynski, I., Shen, Y., Malicka, J., Gryczynski, Z., 2001, Intensified fluorescence, Photon. Spectra, 96–104.
Lawandy, N.M., 2004, Localized surface plasmon singularities in amplifying media, Appl. Phys. Lett. **85**, 540–542.
Lawandy, N.M., 2005, Nano-particle plasmonics in active media, in: McCall, M.W., Dewar, G., Noginov, M.A. (Eds.), Proceedings of SPIE Complex Mediums VI: Light and Complexity, vol. 5924, SPIE, Bellingham, WA, pp. 59240G/1–59240G/13.

Linden, S., Enkrich, C., Wegener, M., Zhou, J., Koschny, T., Soukoulis, C.M., 2004, Magnetic response of metamaterials at 100 terahertz, Science **306**, 1351–1353.
Magde, D., Wong, R., Seybold, P.G., 2002, Fluorescence quantum yields and their relation to lifetimes of rhodamine 6G and fluorescein in nine solvents: improved absolute standards for quantum yields, Photochem. Photobiol. **75**, 327–334.
Markel, V.A., Shalaev, V.M., Stechel, E.B., Kim, W., Armstrong, R.L., 1996, Small-particle composites. I. linear optical properties, Phys. Rev. B **53**, 2425–2436.
Melville, D.O.S., Blaikie, R.J., 2005, Super-resolution imaging through a planar silver layer, Opt. Expr. **13**, 2127–2134.
Mock, J.J., Barbic, M., Smith, D.R., Schultz, D.A., Schultz, S., 2002, Shape effects in plasmon resonance of individual colloidal silver nanoparticles, Chem. Phys. **116**, 6755–6759.
Moskovits, M., 1985, Surface-enhanced spectroscopy, Rev. Mod. Phys. **57**, 783–826.
Müller, R., Zander, C., Sauer, M., Deimel, M., Ko, D.-S., Siebert, S., Arden-Jacob, J., Deltau, G., Marx, N.J., Drexhage, K.H., Wolfrum, J., 1996, Time-resolved identification of single molecules in solution with a pulsed semiconductor diode laser, Chem. Phys. Lett. **262**, 716–722.
Nezhad, M.P., Tetz, K., Fainman, Y., 2004, Gain assisted propagation of surface plasmon polaritons on planar metallic waveguides, Optics Express **12**, 4072–4079.
Nie, S., Emory, S.R., 1997, Probing single molecules and single nanoparticles by surface-enhanced Raman scattering, Science **275**, 1102–1104.
Noginov, M.A., Zhu, G., Shalaev, V.M., Drachev, V.P., Bahouza, M., Adegoke, J., Small, C., Ritzo, B. A., 2005a, "Enhancement and suppression of surface plasmon resonance in Ag aggregate by optical gain and absorption in surrounding dielectric medium", arxiv, physics/0601001 (2005).
Noginov, M.A., Zhu, G., Davison, C., Pradhan, A.K., Zhang, K., Bahoura, M., Codrington, M., Drachev, V.P., Shalaev, V.M., Zolin, V.F., 2005b, Effect of Ag aggregate on spectroscopic properties of Eu:Y_2O_3 nanoparticles, J. Mod. Opt. **52**, 2331–2341.
Noginov, M.A., Vondrova, M., Williams, S.N., Bahoura, M., Gavrilenko, V.I., Black, S.M., Drachev, V.P., Shalaev, V.M., Sykes, A., 2005c, Spectroscopic studies of liquid solutions of R6G laser dye and Ag nanoparticle aggregates, J. Opt. A Pure Appl. Opt. **7**, S219–S229.
Noginov, M.A., Zhu, G., Bahoura, M., Adegoke, J., Small, C., Ritzo, B.A., Drachev, V.P., Shalaev, V.M., 2006a, Applied Physics β; published online August 2006.
Noginov, M.A., Zhu, G., Bahouza, M., Adegoke, J., Small, C., Ritzo, B.A., Drachev, V.P., Shalaev, V.M., 2006b, "Enhancement of surface plasmons in Ag aggregate by optical gain in dielectric medium", Optics Letters, in print.
Noginov, M.A., Zhu, G., Bahouza, M., Adegoke, J., Small, C., Darvison, C, Drachev, V.P., Nyga, P., Shalaev, V.M., 2006c, "Enhancement of spontaneous and stimulated emission of rhodamine 6G dye by Ag aggregate", communicated to the journal.
Pendry, J.B., 2000, Negative refraction makes a perfect lens, Phys. Rev. Lett. **85**, 3966–3969.
Pham, T., Jackson, J.B., Halas, N.J., Lee, T.R., 2002, Preparation and characterization of gold nanoshells coated with self-assembled monolayers, Langmuir **18**, 4915–4920.
Plotz, G.A., Simon, H.J., Tucciarone, J.M., 1979, Enhanced total reflection with surface plasmons, JOSA **69**, 419–421.
Podolskiy, V.A., Sarychev, A.K., Narimanov, E.E., Shalaev, V.M., 2005, Resonant light interaction with plasmonic nanowire systems, J. Opt. A Pure Appl. Opt. **7**, S32–S37.
Podolskiy, V.A., Sarychev, A.K., Shalaev, V.M., 2002, Plasmon modes in metal nanowires and left-handed materials, J. Nonlinear Opt. Phys. Mat. **11**, 65–74.
Podolskiy, V.A., Sarychev, A.K., Shalaev, V.M., 2003, Plasmon modes and negative refraction in metal nanowire composites, Opt. Expr. **11**, 735–745.
Prodan, E., Radloff, C., Halas, N.J., Nordlander, P., 2003, A hybridization model for the plasmon response of complex nanostructures, Science **302**, 419–422.

Quinten, M., 1999, Optical effects associated with aggregates of clusters, J. Cluster Sci. **10**, 319–358.

Quinten, M., Leitner, A., Krenn, J.R., Aussenegg, F.R., 1998, Electromagnetic energy-transport via linear chains of silver nanoparticles, Opt. Lett. **23**, 1331–1333.

Ritchie, R.H., 1973, Surface plasmons in solids, Surf. Sci. **34**(1), 1–19.

Ritchie, G., Burstein, E., 1981, Luminescence of dye molecules adsorbed at a Ag surface, Phys. Rev. B **24**, 4843–4846.

S'anchez, E.J., Novotny, L., Xie, X.S., 1999, Near-field fluorescence microscopy based on two-photon excitation with metal tips, Phys. Rev. Lett. **82**, 4014–4017.

Schaadt, D.M., Feng, B., Yu, E.T., 2005, Enhanced semiconductor optical absorption via surface plasmon excitation in metal nanoparticles, Appl. Phys. Lett. **86**(063106), 3.

Seidel, J., Grafstroem, S., Eng, L., 2005, Stimulated emission of surface plasmons at the interface between a silver film and an optically pumped dye solution, Phys. Rev. Lett. **94**(177401), 1–4.

Selanger, K.A., Falnes, J., Sikkeland, T., 1977, Fluorescence life-time studies of Rhodamine 6G in Methanol, J. Phys. Chem. **81**, 1960–1963.

Selvan, S.T., Hayakawa, T., Nogami, M., 1999, Remarkable influence of silver islands on the enhancement of fluorescence from Eu^{3+} ion-doped silica gels, J. Phys. Chem. B **103**, 7064–7067.

Shalaev, V.M., 1996, Electromagnetic properties of small-particle composites, Phys. Reports **272**, 61–137.

Shalaev, V.M., 2000, Nonlinear Optics of Random Media: Fractal Composites and Metal-Dielectric Films, Springer Tracts in Modern Physics, vol. 158, Springer, Berlin, Heidelberg.

Shalaev, V.M. (Ed.), 2002. Optical Properties of Random Nanostructures, Topics in Applied Physics vol. 82, Springer Verlag, Berlin, Heidelberg.

Shalaev, V.M., Cai, W., Chettiar, U., Yuan, H.-K., Sarychev, A.K., Drachev, V.P., Kildishev, A.V., 2005, Negative index of refraction in optical metamaterials, Opt. Lett. **30**, 3356–3358; arXiv:physics/0504091, Apr. 13, 2005.

Shalaev, V.M., Poliakov, E.Y., Markel, V.A., 1996, Small-particle composites. II. Linear optical properties, Phys. Rev. B **53**, 2437–2449.

Shelby, R.A., Smith, D.R., Schultz, S., 2001, Experimental verification of a negative index of refraction, Science **292**, 77–79.

Smith, D.R., Padilla, W., Vier, J.D.C., Nemat-Nasser, S.C., Schultz, S., 2000, Composite medium with simultaneously negative permeability and permittivity, Phys. Rev. Lett. **84**, 4184–4187.

Stockman, M.I., 1989, Possibility of laser nanomodification of surfaces with the use of the scanning tunneling microscope, Optoelectron. Instrument Data Process **3**, 27–37.

Stockman, M.I., 2005, Ultrafast, nonlinear, and active nanoplasmonics, in: McCall, M.W., Dewar, G., Noginov, M.A. (Eds.), Proceedings of SPIE Complex mediums VI: Light and Complexity, vol. 5924, SPIE, Bellingham, WA, pp. 59240F/1–59240F/12.

Su, K.-H., Wei, Q.-H., Zhang, X., Mock, J.J., Smith, D.R., Schultz, S., 2003, Interparticle coupling effects on plasmon resonances of nanogold particles, Nano Lett. **3**, 1087–1090.

Sudarkin, A.N., Demkovich, P.A., 1989, Excitation of surface electromagnetic waves on the boundary of a metal with an amplifying medium, Sov. Phys. Tech. Phys. **34**, 764–766.

Svelto, O., 1998, Principles of Lasers, 4th ed., Plenum Press, New York.

Veselago, V.G., 1968, The electrodynamics of substances with simultaneously negative values of ε and μ, Soviet Physics Uspekhi **10**(4), 509–514.

Weitz, D.A., Garoff, S., Gersten, J.I., Nitzan, A., 1983, The enhancement of Raman scattering, resonance Raman scattering, and fluorescence from molecules absorbed on a rough silver surface, J. Chem. Phys. **78**, 5324–5338.

Yen, T.J., Padilla, W.J., Fang, N., Vier, D.C., Smith, D.R., Pendry, J.B., Basov, D.N., Zhang, X., 2004, Terahertz magnetic response from artificial materials, Science **303**, 1494–1496.

Zander, C., Sauer, M., Drexhage, K.H., Ko, D.-S., Schulz, A., Wolfrum, J., Brand, L., Eggelin, C., Seidel, C.A.M., 1996, Detection and characterization of single molecules in aqueous solution, Appl. Phys. B Lasers Opt. **63**, 517–523.

Zhang, S., Fan, W., Minhas, B.K., Frauenglass, A., Malloy, K.J., Brueck, S.R.J., 2005, Midinfrared resonant magnetic nanostructures exhibiting a negative permeability, Phys. Rev. Lett. **94**(037402), 1–4.